

Chemical Engineering

Principles of Plasma Processing

UCLA, Spring 2004

Due: April 29, 2004

(From HW#2)

5. Determine the gas flow regimes and calculate the mean free paths of the N_2 gas molecules at (1) 0.1 mtorr, 300K and (2) 10 torr, 700K. Assume the characteristic length of the process chamber is 5 cm.

1. A gas flow of 2 sccm is introduced into a plasma chamber through a 5 cm short circular tube which is 1" in diameter. The chamber is pumped by a turbo pump with a pumping speed of 500l/s, which is backed by a roughing pump with a pumping speed of 30 cfm. A throttle valve is installed to control the pressure of the reactor. The conductance of the throttle valve as a function of its opening in percentages ($\beta\%$) as: $C_{\text{valve}}=75\times\beta\%+25\times(\beta\%)^2$ [l/s]. Assume that the gas has the flow characteristics of air. What is the flow regime as the valve opens from 0.1% to 100%? Find out the pressure response as the opening of the throttle valve and calculate the lower limit of the pressure. Find out the base pressure of this system if the system leak is on the order of 0.001 sccm.

2. Determine the ground state levels for Si, O, F, Cl, Ar, and Ti. Show how each of the "labels" used in the spectroscopic terms of atoms is determined.

3. (1) Following the Thomson procedure, estimate the ionization cross-section per valence electron from the metastable $n=2$ level, having an energy $E_2=E_{iz}/4$. (2) Find the ratio of the maximum metastable to ground-state Thomson ionization cross-sections. (3) Using the Thomson formula for ionization cross-section near the threshold energy $E=E_{iz}$, derive the ionization rate constant: $K_{iz}(T_e)=\sigma_0\bar{v}_e\left(1+\frac{2T_e}{E_{iz}}\right)e^{-\frac{E_{iz}}{T_e}}$, where $\bar{v}_e=\sqrt{\frac{8kT}{\pi m}}$. (4) Find the ratio of the maximum metastable to ground-state ionization rate constant if $E_{iz}=15.8$ eV and $T_e=4$ eV.

4. Use Fig. 20 on page 149 in the textbook, identify and discuss the dissociation, dissociative ionization, dissociative recombination, dissociative electron attachment, and polar dissociation processes. Label the pertinent energies on the diagram and discuss the energy of the dissociated atoms, whenever possible.

5. Problem 8. 7 in LL.

** Hand in a copy of the reference assigned to you in Meeks and Ho's paper (assignment on the back of this page).

Hand in a copy of the reference assigned to you in Meeks and Ho's paper (assignment on the back of this page).

Last name First name Find the following reference(s) in Meeks and Ho's paper

Burri	Jeremy	27
Cross	Kimberly	28+35
Chairunas	Ivan	29
Lall	Anshuman	30+31
Martin	Ryan	32
Ramirez	Desiree	33
Sawkar	Monica	34
Ta	Yen	36
Tanner	Carey	41
Torreblanca	Humberto	42
Woo	Robyn	43

Modeling plasma chemistry for microelectronics manufacturing

Ellen Meeks^{a,*}, Pauline Ho^b

^aReaction Design, Inc., 6440 Lusk Blvd., Suite D209, San Diego, CA 92121, USA

^bSandia National Laboratories, Albuquerque, NM 87185-0601, USA

Abstract

A methodology is presented for developing and testing plasma chemistry mechanisms needed for numerical models of microelectronics processing technologies. This includes a description of the types of data required for building a kinetic model, common sources for obtaining fundamental and kinetic data, suggestions for estimating kinetic parameters when data are not available, and approaches to validation and tuning of the model using diagnostic and sensor data. The approach focuses on the use of the CHEMKIN Collection software for describing the gas-phase and surface reaction kinetics in high-density plasma simulations. © 2000 Elsevier Science S.A. All rights reserved.

Keywords: Plasma chemistry; Microelectronics; Processor; Numerical model

1. Introduction

Plasma processing has become increasingly important in the microelectronics industry, particularly for the ‘back-end-of-line’ process steps that follow the initial construction of a semiconductor device on a silicon wafer. In the back-end-of-line, existing circuit elements on the wafer can be highly sensitive to subsequent processing environments. The plasma environment offers advantages over thermal processes due to the ability to maintain low wafer temperatures, while achieving high processing rates. The so-called ‘high-density’ plasma (HDP) reactors have an added advantage over traditional plasma diode reactors, by providing the process designer with separate control of ion energy and ion flux [1]. In this way, high processing rates can be maintained without introducing excessive ion-induced damage on the wafer. Important process steps that are now performed routinely by high-density plasma reactors include plasma deposition of inter-metal dielectrics, dielectric etching, poly-silicon etching, metal etching, and photoresist stripping. In addition to process speed and wafer uniformity demands, many of these processes also have stringent microscopic patterning requirements. The ability to anisotropically etch deep, sub-0.5- μm trenches and vias, for example, determines critical performance parameters in the resulting circuit.

The kinetics of the competing chemical reactions that occur within a plasma-deposition or plasma-etch chamber affect almost every metric of the wafer process. Especially in low-pressure (2–20 mTorr) plasma reactors, where trans-

port processes are fast, gas-phase and surface kinetics dominate the determination of etch or deposition rates, etch or deposition uniformity, etch selectivity, and profile evolution. Parasitic chemical reactions, such as wall deposition or wall ‘conditioning’, often control the robustness, reproducibility, and operating margin of a process. In addition to these direct process performance measures, the chemistry occurring in a plasma reactor controls the reactor emissions, the need for abatement of the reactor exhaust, gas-utilization requirements, and the frequency and method of reactor cleaning. These latter effects can be important in determining both direct and indirect costs of reactor usage.

Modeling and simulation, together with experimentation, can provide necessary information about the competing processes in a plasma reactor and allow better control of the process performance. In order for plasma reactor modeling to provide relevant information to reactor and process designers, however, the models must capture the important kinetic phenomena. Although the literature contains much information on fundamental plasma phenomena, insufficient attention has been paid to methods for using this fundamental data in simulating real reactor conditions with complex gas mixtures and surface processes. This article discusses methods for applying appropriate levels of plasma models in engineering simulations and a means of obtaining required input data. The needed chemistry parameters include a gas-phase chemistry mechanism (reaction paths plus rate parameters), a surface chemistry mechanism, and a set of transport-property data (if transport effects are included). A methodology for obtaining these parameters is shown schematically in Fig. 1. A similar discussion of chemical kinetics

* Corresponding author. 304 Daisyfield Drive, Livermore, CA 94550, USA.

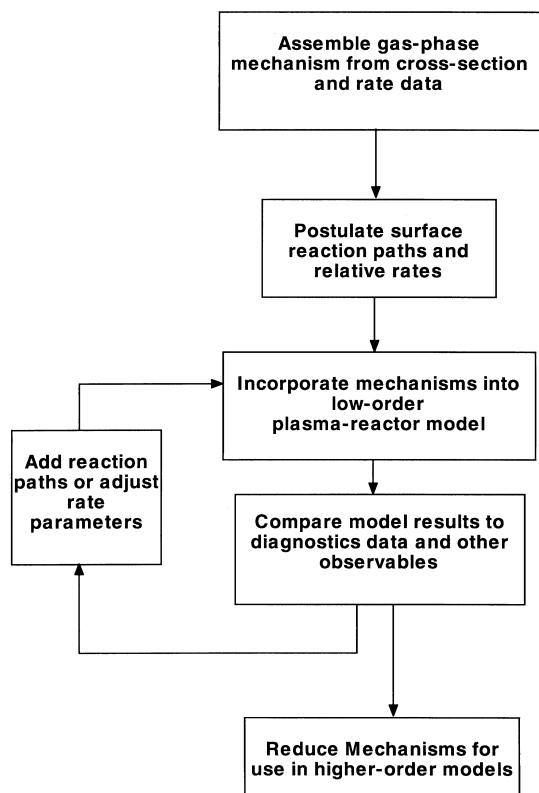


Fig. 1. Flow chart of mechanism-development process for plasma systems.

in non-plasma chemical-vapor-deposition (CVD) reactors is given elsewhere in this journal issue [2].

2. Data requirements for plasma modeling

Successful numerical simulations of real plasma processing systems require compromises between the level of detail included in the model and the computational

resources required. Such compromises often involve trade-offs between the descriptions of transport and chemistry. A simulation that treats transport issues in two or three dimensions will generally include simplified chemistry, while simulations that focus on a detailed description of the reaction kinetics generally use a simplified description of the transport in the reactor. There are several comprehensive reviews of plasma reactor models and modeling techniques [3–6], so only a brief discussion is included here, with an emphasis on the different data requirements for different approaches to plasma modeling summarized in Table 1.

The simplest treatment of the transport in a plasma reactor is the use of ‘global’ or well-mixed-reactor approaches [7–11]. The formulation is similar to that of a perfectly stirred reactor (PSR) or continuously stirred tank reactor (CSTR), commonly used in chemical engineering. These compact models assume fast transport and focus instead on the competing kinetic processes. They typically provide no information about etching or deposition uniformity, but are computationally very fast. Such models are useful in providing first-cut understanding of plasma behavior and as tools for developing and testing reaction mechanisms. They require rate coefficients and thermodynamic data for the electron-impact, neutral and ion reactions of interest both in the gas-phase and at the surface.

Continuum models have been successfully applied to the plasmas used for microelectronics processing [12–17], even though the pressures are below the range where continuum models of transport are generally considered reliable. In view of the fact that transport processes are typically not rate limiting for either etching or deposition in an HDP reactor, the approximate description of the transport phenomena provided by the continuum models often suffices, despite the large Knudsen numbers that characterize the reactor. In addition to a description of the chemistry, these models require transport properties for all the gas-phase species of interest.

Table 1
Data requirements for different plasma modeling approaches

	Well mixed reactor models	Continuum models	Models with Monte Carlo neutrals and ions, and continuum electrons	Models with continuum neutrals and ions, and Monte Carlo electrons
Electron-impact cross sections				×
Electron-impact reaction-rate coefficients	×	×	×	
Neutral and ion rate coefficients	×	×	×	×
Fundamental transport parameters (e.g. Lennard–Jones parameters)			×	
Transport-properties (e.g. thermal conductivity, viscosity, diffusion coefficients)		×	× (electrons)	× (neutrals and ions)
Thermodynamic data	×	×	×	×
Surface reaction rates and probabilities	×	×	×	×

Despite the success of the continuum models, the very low pressures ($\sim 2\text{--}20$ mTorr) suggest that a non-continuum approach more accurately describes the transport phenomena in the reactor. To this end, several groups have developed direct-simulation Monte Carlo (DSMC) models for plasma-reactor simulation [18–21]. Although a Monte Carlo or other particle approach to transport modeling implies the direct use of collision cross sections, such detailed information for heavy-body collisions is often difficult to find. In practical DSMC implementations, therefore, cross sections are often derived from reaction-rate coefficients [22]. In this way, the input data requirements are not substantially different from those of a continuum model.

For models that include a kinetic description of the electrons, however (see, for example Venzek et al. [12]), electron cross sections are employed directly in the model. Such models typically solve the Boltzmann equation, either directly or through Monte Carlo techniques, to determine local electron-energy distribution functions. This information, together with the energy-dependent cross sections, allows determination of local reaction rates that depend not only on the mean electron energy but also on the local field and gas composition.

3. Assembling the gas-phase plasma mechanism

The approach to developing gas-phase mechanisms described here focuses on the use of a continuum description for electron energy and transport and, more specifically, on models employing the CHEMKIN Collection software [23] in the treatment of the plasma reaction kinetics. The CHEMKIN software is a collection of programs and subroutine libraries that facilitate the formation, solution, and interpretation of problems involving homogeneous (gas-phase) and heterogeneous (gas-surface) chemical kinetics. It has recently been extended for application to plasma kinetics and plasma-surface interactions. The method described here will include the transformation of electron collision cross sections to electron-temperature-dependent reaction-rate coefficients. This approach has been applied in well-mixed reactor modeling [9,17,24] as well as in continuum [17] and DSMC [25] plasma-transport models.

Development of the gas-phase mechanism is an iterative process. It starts with reactions involving the initial reagent gases and then gradually expands to include reactions involving molecule fragments and surface-reaction byproducts. A low-pressure gas-phase plasma mechanism typically comprises a large set of electron-impact collisions as well as fast reactions between neutral radicals, ion–neutral and ion–ion reactions. Recombination processes that involve third-body stabilizations are usually negligible at these mTorr pressures; instead, surface recombination dominates for both ions and neutrals.

One way to select reaction paths to include in a simulation is to begin with available cross-section data for the reagent

gases, and then add new paths that seem likely, given the initial simulation results. Such scoping simulations are best performed with a computationally fast plasma model, such as a well-mixed reactor model [9,23]. Initial simulations identify what molecule fragments and atomic species predominate in the plasma. Adding ionization, dissociation, and vibrational excitation cross sections for these fragments to a new round of simulations then determines a further set of additional species. For typical HDP conditions, it is reasonable to continue the iterative cycle of adding reactions until the fragmentation paths reach the atomic level. For diatomic molecules this is clearly a much simpler process than for a larger polyatomic molecule such as C_4F_8 .

In modeling a plasma process, it is better to include an estimate of a cross section than to neglect probable reaction paths. A nontrivial part of estimating cross-section data is determining the most likely dissociation paths. In the absence of any other information (such as appearance potentials), the weakest bond or the exothermicity of a reaction path can often be used as a guess for the most likely dissociation path.

3.1. Electron-impact reactions

Compilation begins with the collection of available electron-impact cross sections, starting with electrons impacting the reagent molecules. There are a multitude of possible electron-impact excitation processes that occur for any target molecule, but mechanism development must focus on those collisions that are most likely to affect wafer-level processes (i.e. deposition and etching) for the appropriately low electron energies. Fig. 2 shows an example of a ‘complete’ set of electron-impact energy-dependent cross sections that have been compiled for molecular oxygen [24].

The mean electron energy that drives ionization and

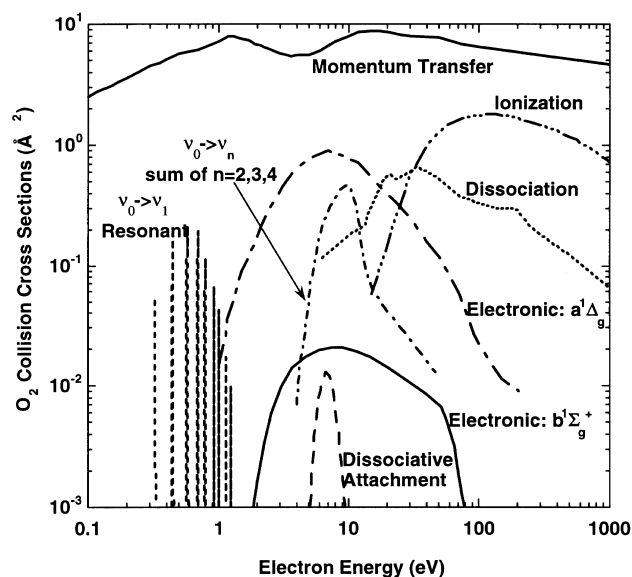


Fig. 2. Example of a cross-section set for molecular oxygen.

dissociation processes is determined from a balance between the plasma power source and collisional energy losses. Consideration of all processes that provide significant energy loss for the electrons is necessary, but this does not mean that all possible processes need to be included. For O_2 , Fig. 2 includes data for electronic excitation to the $^1\Delta_g$ and $b^1\Sigma_g^+$ states, but not all the higher excited states. Data for the electron-induced vibrational excitation of O_2 are explicitly included as a resonant process for $\nu = 0 \rightarrow \nu = 1$, but are included as an averaged sum of the excitations to the next three higher vibrational states. Cross sections for momentum-transfer processes, which are important for spatially dependent simulations and will be discussed in more detail in Section 5, are also included in Fig. 2. For molecules, the dominant energy-loss process is usually vibrational excitation, while electronic excitations dominate for atomic species.

Plasma-enhanced etch and deposition chemistry depend on the identity and fluxes of ions and radicals from the plasma to the wafer surface. Therefore, processes such as ionization, dissociative ionization, and excitation leading to neutral dissociation are of first-order importance. As electron energies are relatively low, we rarely consider multiply ionized states. Thus, Fig. 2 includes a single electron-induced ionization process for O_2 . Likewise, the simplicity of O_2 results in only one dissociation process being included, although the formation of electronically excited O atoms (particularly metastables) may be important. A more complex polyatomic molecule is likely to have a number of dissociation reactions. Finally, since many of the typical process gases have electro-negative properties, it is often important to consider electron attachment, dissociative attachment (included in Fig. 2), and detachment reactions.

Especially for complex systems, the lack of fundamental data, including electron-collision cross sections, is a common obstacle for plasma modelers. A workshop sponsored by the National Research Council in 1995 focused on database needs for modeling and simulation, and resulted in a priority list of chemistries deemed to be most critical to the microelectronics industry [26]. The processes targeted were (1) poly-silicon etching, involving Cl_2 , Br_2 , HBr , O_2 , and N_2 ; (2) silicon dioxide etching involving CF_4 , CHF_3 , C_2F_6 , O_2 , N_2 , CO , and Ar ; and (3) silicon dioxide deposition, involving SiH_4 , O_2 , N_2O , Ar , and $TEOS$. Several compilations of cross sections for relevant molecules are already available, and are listed in Table 2. Critical reviews provide some measure of the uncertainty in the cross sections as well as the data values. In other cases, sets of electron cross sections have been reported in the context of plasma reactor modeling, where the validation of the cross-section set is indirect through the ability of the plasma model to reproduce macroscopic effects measured in an actual reactor.

Other sets of data are available in the literature. For example, Bell et al. [42], Lennon et al. [43], and Freund et al. [44] present atomic ionization cross sections. Several books have been published that contain cross-section data of common

molecules, such as rare gases and species that occur in the atmosphere [45,46]. Semi-empirical or semi-classical formulas for estimating some cross sections, particularly for ionization, are reviewed by Christophorou [46].

Finally, one can access more current data through bibliographic databases that are accessible via the internet, such as GAPHYOR (GAZ-PHYsics-ORsay) Data Center, located in Orsay at the Laboratoire de Physique des Gaz et des Plasmas [47]. Online databases of the cross-section values themselves are growing in popularity and content, such as those provided by the National Institute of Standards and Technology [48], Kinema Research, Inc. [49], and NASA Ames [50].

Despite these recent advances and efforts to accommodate the needs of modelers by providing reviewed sets of cross sections, the modeler must often make some estimates for molecules where little or no fundamental information is available. Target chemistries can change rapidly in the microelectronics industry and new chemical additives are often used to modify existing processes. In addition, difficulties in measurement or computation of certain cross sections may preclude their availability.

It is often possible to estimate cross-section data based on information about the structure and energetics of the species, and on information available from species of similar structure or energetics. Cross sections for classes of processes, such as ionization, dissociation, and vibrational excitation, tend to have similarly shaped dependencies on electron energy, and can be characterized roughly by the energy threshold and by the peak cross-section values. Taking a known cross section from a 'similar' molecule and then scaling the threshold and peak values is therefore a reasonable way to arrive at estimates for unknown data. Here 'similar' may mean similar structure, e.g. SiH_4 is similar to CH_4 , or having similar bonds, e.g. BCl_2 is similar to BCl_3 . However, one must be cautious in this approach, since analogous ions may not exist; for example, CH_4^+ ion exists, while SiH_4^+ does not.

The energy threshold of the cross section is a measure of the electron energy required for the process to proceed. The obvious scaling factor for ionization cross sections is the ionization potential of the molecule. Ionization potentials for various species are reported, for example, in the NIST Structures and Properties Database [51]. For a dissociation process, a reasonable approximation for the minimum energy threshold is the net change in enthalpy of the process, or the heat of reaction, which is readily calculated from species' heats of formation [51,52]. Note, however, that dissociation thresholds can be significantly larger than the exothermicity calculated in this manner. For excitations, energy thresholds are roughly the difference between the excited and ground-state energy levels. Electronic and vibrational excitation energies of various species are reported, for example, in the JANAF tables [52] or in compilations of spectroscopic data (see, for example, Huber and Herzberg [53]). In the absence of specific data, it is sometimes assumed that all electronic excitations in

Table 2
 Compilations of electron-impact cross-section data

Molecule	Authors	Year	Comments
CF ₄	Christophorou et al. [27]	1996	Critical review
CF ₄	Morgan [28]	1992	Critical review
C ₂ F ₆	Christophorou et al. [29]	1998	Critical review
CHF ₃	Christophorou et al. [30]	1997	Critical review
CCl ₂ F ₂	Christophorou et al. [31]	1997	Critical review
C ₃ F ₈	Christophorou et al. [32]	1998	Critical review
O ₂	Itikawa [33]	1989	Critical review with some estimates; more recent data available for O ₂ dissociation [32]
O	Itikawa [34]	1990	Critical review with some estimates
Cl ₂	Morgan [35]	1992	Critical review
F ₂	Morgan [35]	1992	Critical review
HCl	Morgan [35]	1992	Critical review
SiH ₄	Perrin [36]	1996	Critical review
SiH ₄	Morgan [28]	1992	Critical review
CH ₄	Morgan [28]	1992	Critical review
H ₂	Janev, et al. [37]	1987	Critical review
H	Janev, et al. [37]	1987	Critical review
SF ₆	Phelps and Van Brunt [38]	1988	Critical review
He/N ₂ /O ₂	Sommerer and Kushner [39]	1992	Validated through comparisons with reactor data
He/CF ₄ /O ₂			
SiH ₄ /NH ₃			
Ar/Cl _x	Bukowski, et al. [40]	1996	Validated through comparisons with reactor data
NF _x /O _x /F _x	Meeks et al. [41]	1997	Validated through comparisons with reactor data
SiH _x /O _x /Ar/H _x	Meeks et al. [24]	1998	Validated through comparisons with reactor data
BCl _x /Cl _x /Ar	Meeks et al. [17]	1998	Validated through comparisons with reactor data

molecules lead to dissociation [27,33]. For molecular ionization, Christophorou [46] suggests that ions with unpaired electrons will tend to be unstable, resulting in a dissociative ionization.

In addition to scaling the threshold, the peak cross-section value may also be scaled according to the probability of the electron colliding with the molecule. Scattering or elastic cross sections can provide this information, if they are available for both the ‘known’ molecule and the ‘estimated’ molecule. In the absence of such data, the peak cross-section values can be scaled either according to polarizability (for polar molecules) or according to size (e.g. Lennard–Jones diameter) of the target molecule.

3.2. Incorporating electron-impact cross sections into continuum models

Plasma models that have a continuum treatment of the electron transport and energy [9,13,14,16–18] employ reaction rates that depend on the mean electron energy. Electron-collision cross sections $\sigma(\varepsilon)$ are converted to reaction rate coefficients through the following integration

$$k = \int_0^{\infty} f(\varepsilon) \left(\frac{2\varepsilon}{m_e} \right)^{1/2} \sigma(\varepsilon) d\varepsilon \quad (1)$$

where k is the reaction-rate coefficient, $f(\varepsilon)$ is the electron energy distribution function (EEDF), and m_e is the electron mass. This integration is straightforward, provided that one knows the form of the EEDF. In that case, the mean electron temperature is determined as

$$T_e = \frac{2}{3} \frac{\bar{\varepsilon}}{k_B} = \frac{2}{3k_B} \int_0^{\infty} \varepsilon f(\varepsilon) d\varepsilon \quad (2)$$

where k_B is the Boltzmann constant.

However, an accurate determination of the local EEDF requires a spatially dependent kinetic simulation, either through particle treatment of the electrons or through direct solution of the Boltzmann equation. Ideally such a treatment would couple the determination of local plasma conditions (e.g. composition, percent ionization) and electrodynamics with the calculations of kinetic rates. This approach is computationally prohibitive in most practical cases, and many modelers instead use a form of the EEDF that will allow an a priori determination of $k(T_e)$, where T_e is found through solution of an electron energy equation.

The simplest approach to treating the electron kinetics is to assume a Maxwellian distribution function that is related directly to the mean electron temperature. Other approaches to approximating the EEDF have included solving the Boltzmann equation in advance over a range of conditions to correlate reaction rates and electron temperatures [9] and solving an approximate form of the Boltzmann equation coupled to a well-mixed reactor model [54]. The use of a Maxwellian distribution assumes steady-state equilibrium conditions and neglects effects of inelastic collisions on the distribution function. The inaccuracies of this approach are generally overwhelmed by the uncertainties in the reaction cross sections, except for a few special cases, such as rare gases. For this reason, and because the computational efficiency and simplicity of the approach provides a path for

achieving fast engineering results, Maxwellian distribution functions have been used extensively in modeling HDP systems [8,9,13–19,40]. Assuming a Maxwellian EEDF, Eq. (1) becomes

$$k = \left(\frac{8}{\pi m_e}\right)^{1/2} \left(\frac{1}{k_B T_e}\right)^{3/2} \int_0^\infty \varepsilon \sigma(\varepsilon) e^{-\varepsilon/k_B T_e} d\varepsilon \quad (3)$$

Once the relationship between k and T_e is established, use of the CHEMKIN suite of software requires this function to be reduced to a set of fit coefficients. The default form for fitting coefficients in CHEMKIN is the modified Arrhenius form

$$k(T_e) = AT_e^B \exp\left(\frac{C}{T_e}\right) \quad (4)$$

For some reactions, the functional dependence of the collisional cross section on electron energy is complex, such that a good fit using Eq. (4) is difficult. In such cases, a variety of other rate expressions are available. Alternatively, the fit to the Arrhenius form could be made more accurate by limiting it to a smaller temperature range based on knowledge of the targeted reactor process.

3.3. Neutral reactions

Electron-impact reactions in HDP reactors result in the generation of large concentrations of radical neutral species that ultimately participate in the etching or deposition processes at the wafer. In addition to these surface reactions (addressed below), however, these neutral species may also react in the gas phase. The low pressures of HDP systems place all collision-activated unimolecular decomposition and third-body-stabilized recombination reactions well into their pressure-dependent regimes. Inclusion of such reactions requires full description of the pressure-falloff behavior, and use of reaction rates measured only at high pressures is incorrect. Incorporation of pressure fall-off behavior in neutral kinetics can be done using standard techniques [55,56]. To first order, however, it is reasonable to neglect these reactions because of the very low pressures. In contrast, other types of gas-phase reactions can be important under HDP conditions. Atom-transfer reactions involving radicals (such as H, O, OH, BCl or CF₂), for example, can be quite fast and therefore relevant even at very low pressures [17,24]. Excited state and metastable species can be more reactive than ground-state species and can therefore be important despite their relatively low densities. However, information about reactions involving excited states is often more difficult to find than data involving ground state species. Photochemical reactions are not likely to be important in typical HDP reactors, despite the light emission from plasma discharges.

Data for individual neutral reactions are often available in the literature or from data compilations, such as the NIST Kinetics Database [57,58]. When such information is not available, estimates of reaction rates may be based on simi-

lar types of reactions, on estimates of energy thresholds, and on estimates of molecular collision rates. As an example of the former, an experimental value for rate of the $\text{AlCl} + \text{Cl}_2 \rightarrow \text{AlCl}_2 + \text{Cl}$ reaction is used as an estimated reaction rate for the analogous $\text{BCl} + \text{Cl}_2 \rightarrow \text{BCl}_2 + \text{Cl}$ reaction [17].

3.4. Ion reactions

Ion–neutral and ion–ion reactions also play significant roles in the plasma chemistry of an HDP reactor. Mutual neutralization between positive and negative ions are an important loss term for ions in an electronegative discharge. In general, the dominant positive ion in the discharge is expected to be that of the molecule or atom of the lowest ionization potential, provided it is also of sufficient abundance in the plasma. Charge-exchange reactions help to determine the identity of the dominant ion in the discharge. These reactions also provide a route for energy exchange between the charged and the neutral species.

Most of the available rate data for ion-driven reactions arises from studies of atmospheric or astronomical chemistry. While such measurements were performed under significantly different conditions from a wafer-processing plasma, they provide some indication of probable reaction paths and typical reaction rate coefficients for relevant processes. Anicich reviewed ion reactions relevant to atmospheric chemistry in 1993 [59]. Other reports of ion–neutral reaction rates include works by Farrar [60], Phelps [61], and Kickel et al. [62]. Mass spectrometric measurements of charge exchange reactions are often included in reports of electron-impact cross sections for chemistries more directly relevant to microelectronics (see for example Jiao et al. [63,64] or Perrin et al. [36]).

Negative ion reactions, such as mutual neutralization with positive ions or associative detachment reactions, are discussed by Smirnov [65]. Smirnov derives a formula for estimating mutual neutralization rate coefficients, as follows

$$k = 7 \times 10^{-6} / \sqrt{\varepsilon_A T_i \mu} \quad (5)$$

where ε_A is the electron-binding energy for the negative ion in electron volts, T_i is the ion temperature in Kelvin, and μ is the reduced mass of the colliding ions in units of proton mass (the mass of a proton = 1.673×10^{-24} g). The validity of Eq. (5) is given as within 30% for ion temperatures much less than $2 \times 10^4 \sqrt{\varepsilon_A}$ [65]. Smirnov also provides tables of measured detachment reaction rates, as well as correlations of these rates with the energy deficit for the reaction path.

3.5. Thermodynamic properties

Thermodynamic properties for each chemical species are employed in plasma simulations in several ways. First, heat capacities of the species are required to determine the mixture specific heat when solving the (transient) neutral-gas energy equation. Second, the enthalpy of each species is required to determine the heat of reaction for the inelastic

processes. The enthalpy gain or loss due to chemical reactions can be important terms in both the neutral-gas and the electron energy equations. In the CHEMKIN software, one can explicitly supply the energy loss per reaction event, but by default the energy loss is calculated from the relative species enthalpies [23]. Third, although most gas-phase electron-driven reactions under HDP conditions are written as irreversible processes, neutral reactions are usually reversible. The reverse rates are calculated by way of an equilibrium constant for each reaction, which is determined from the enthalpy and entropy of the species involved.

For many gas-phase neutral species, thermodynamic properties can be obtained from standard compilations such as the CHEMKIN thermodynamic database [23], the JANAF thermodynamic tables [52], the NASA Lewis thermodynamic database [66] or in recent years, from quantum chemical calculations [67–70]. For some ions, these sources also provide thermodynamic information. For many ions and excited-state species, however, it is often necessary to estimate thermodynamic data. A reasonable approach to estimating positive-ion properties is to start with the raw data for the corresponding neutral species in the form of specific heat, enthalpy, and entropy as a function of temperature. Adding the ionization potential to the species heat of formation and the absolute enthalpy values produces an estimate of the ion's enthalpy as a function of temperature. To a first approximation, the specific heat and entropy remain unchanged from the corresponding neutral. We make similar estimates for excited species or negative ions by adding the excitation energy to or subtracting the electron affinity from the neutral heat of formation, respectively [24].

3.6. Example gas-phase chemistry mechanism

Table 3 provides an example of a gas-phase chemistry reaction set for oxygen plasmas under HDP conditions. This data was generated using the approach described above, and the mechanism was validated as part of a detailed study of $\text{SiH}_4/\text{O}_2/\text{Ar}$ plasma deposition of SiO_2 [24]. References to the individual reactions in Table 3 are provided elsewhere [24]. The reaction set includes electron-impact reaction rates that were derived from the electron-impact cross sections in Fig. 2, assuming a Maxwellian EEDF. Table 3 also includes examples of charge-exchange (Reaction 21), associative electron detachment (Reaction 20), and fast neutral-radical reactions (Reactions 22, 23), as well as ion-ion mutual neutralization reaction rates based on measured data (Reactions 18, 19).

4. Assembling the surface chemistry mechanism

Developing a self-consistent set of reactions to describe the plasma-surface interactions in a reactor is much less straightforward than for the gas-phase. It is also an iterative process and must be done in synchronization with development of the gas-phase reaction mechanism because surface

reactions can provide large production or loss terms for gas-phase species. Thus, the surface chemistry mechanism needs to be an integral part of all stages of the process of sorting out dominant and negligible reaction paths.

The methodology of the CHEMKIN Collection software for describing the heterogeneous kinetics allows the specification of a variety of surface species and inclusion of both chemically driven and ion-induced surface reactions, including adsorption, desorption, and reactions between different surface species. Elementary chemical reaction steps may be treated separately or lumped together as an effective process. The formalism defines a surface species as a chemical species at the boundary between the solid material and the gas, e.g. an adsorbate. Each surface species occupies one or more 'sites' and the total number of sites is usually conserved. 'Bulk' species are entities in the solid phase that may be created or destroyed due to the deposition or to etch of the bulk material 'below' the surface layer. In addition, the software allows consideration of different reaction sets on different materials in the reactor, for example wall chemistry and wafer chemistry. Details regarding this software and formalism are available elsewhere [2,71–73].

For HDP etching and deposition processes, several classes of reactions that may be included in the surface reaction mechanism are shown schematically in Fig. 3. Important processes include ion neutralization on all surfaces, thermal or chemically driven reactions involving neutral radicals, ion-enhanced chemical reactions, and physical ion sputtering. Such plasma-surface interactions for low-temperature plasmas have been reviewed elsewhere by Coburn and Winters [74,75], Hess [76], and Oehrlein [77]. Classifying surface reactions is useful in assigning initial rates or reaction probabilities to the reaction paths. For example, in the absence of experimental data, all ions might be estimated to have the same yield coefficient, or one that scales with ion mass. Likewise, all radicals might be assumed to 'stick' with the same fixed probability, or one that scales with the degree of unsaturation in the radical.

Surface science experiments, especially those applied to environments similar to the actual plasma reactor environment, provide essential information for deriving plasma-surface reaction mechanisms. Oehrlein recently reviewed such experiments for plasma processing systems [77]. Relevant techniques include analyses of incident and outgoing species fluxes to the surface, measurements of deposition thickness and composition, and experiments that identify the chemical nature, including coverage and bonding, of surface species. Another method for sorting among competing processes on wafer surfaces, is to build special microscopic structures on a test wafer that are designed to separate competing effects. For example, Cheng et al. [78] used test structures to separate the contributions due to direct deposition from gas precursors from those due to 're-deposition' of sputtered fragments in a gap-fill process.

The surface reaction mechanism ultimately reflects the depth and breadth of the state of scientific understanding

Table 3

Gas-phase mechanism for O₂ plasmas [24]: rate coefficients in form $k_f = AT^B \exp(-C/T)$; units are molecules, centimeters, seconds, and Kelvin

Reaction	A	B	C	Notes
<i>Electron-impact reactions</i>				
1. E + O ₂ → O ₂ + E	1.41×10^{-4}	-1.5	11594.0	$\nu_0 \rightarrow \nu_1^a$
2. E + O ₂ → O ₂ + E	2.41×10^{-4}	-0.9	76827.0	$\sum_{n=2,3,4} (\nu_0 - \nu_n)^a$
3. E + O ₂ → O ₂ + E	7.13×10^{-8}	-0.1	30812.0	$a^1 \Delta_g^b$
4. E + O ₂ → O ₂ + E	2.75×10^{-10}	0.0	30656.0	$b^1 \Sigma_g^{+b}$
5. E + O ₂ → O ₂ + E	2.29×10^{-10}	0.4	68652.0	$B^3 \Sigma_u^- + A^3 \Sigma_u^+ + C^3 \Delta_u + c^1 \Sigma_u^-b$
6. E + O ₂ → O + O* + E	4.52×10^{-13}	0.9	51069.0	
7. E + O ₂ → O ₂ ⁺ + 2E	3.99×10^{-14}	1.1	137580.0	
8. E + O ₂ → O + O ⁻	3.60×10^{-8}	-0.5	57440.0	
9. E + O → O* + E	4.30×10^{-7}	-0.3	38431.0	$2p^4 \ ^1D^b$
10. E + O → O + E	1.24×10^{-9}	0.0	60440.0	$2p^4 \ ^1S^b$
11. E + O → O + E	1.67×10^{-9}	0.0	146940.0	$3s^2 \ ^3D^{0b}$
12. E + O → O + E	4.36×10^{-9}	0.0	110150.0	$3s^2 \ ^3S^{0b}$
13. E + O → O + E	1.93×10^{-15}	1.1	530780.0	O ^{++b}
14. E + O → O ⁺ + 2E	1.95×10^{-11}	0.6	165410.0	
15. E + O* → O ⁺ + 2E	1.95×10^{-11}	0.6	140000.0	c
16. E + O ⁻ → O + 2E	2.10×10^{-10}	0.5	39434.0	
17. E + E + O → O ⁻ + E	1.00×10^{-30}	0.0	0.0	
<i>Ion reactions</i>				
18. O ⁻ + O ₂ ⁺ → O + O ₂	2.80×10^{-7}	0.0	0.0	d
19. O ⁻ + O ⁺ → 2O	2.80×10^{-7}	0.0	0.0	
20. O ⁻ + O → O ₂ + E	1.40×10^{-10}	0.0	0.0	
21. O ⁺ + O ₂ → O ₂ ⁺ + O	2.10×10^{-11}	0.0	0.0	
<i>Neutral reactions with O*</i>				
22. O* + O ₂ → O + O ₂	3.20×10^{-11}	0.0	-67.0	
23. O* + O → O + O	4.00×10^{-11}	0.0	0.0	

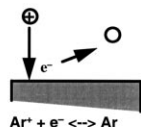
^a This reaction is a vibrational excitation, for which the excited state is indicated in the Notes column.

^b This reaction is an electronic excitation, for which the excited state is indicated in the Notes column.

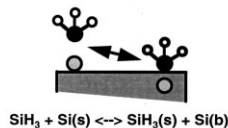
^c The reaction-rate parameters are estimated from Reaction 14.

^d The reaction-rate parameters are estimated from Reaction 19.

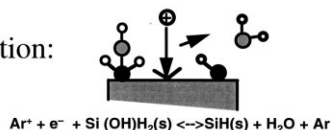
Ion Neutralization:



Radical Adsorption / Deposition:



Ion-enhanced Reaction:



Physical Ion Sputtering:

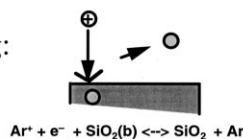


Fig. 3. Schematic representation of classes of surface reactions important to HDP etching and deposition.

about the etch or deposition process. In other words, the complexity of the model should not exceed the knowledge base. Lack of fundamental data for individual processes will therefore result in more global reaction descriptions. The surface chemistry description allows postulation and testing of hypotheses against observables as the knowledge base grows. With reaction mechanisms incorporated into a reactor model, we also use macroscopic data, such as etch or deposition rate, to explore rate-limiting steps. Trends in macroscopic data often reveal missing reaction paths or dependencies. For example, in the study of oxide deposition from SiH₄/O₂/Ar plasmas, data showing an increase in deposition rate as a function of oxygen addition suggested that the O atom incorporation into the bulk oxide was a rate-limiting step under the conditions being studied [24].

4.1. Ion neutralization

For low-pressure plasma systems, positive-ion recombination with electrons on surfaces represents the major loss path for charged species. For this reason, appropriate rates for ion neutralization must be included on all surfaces in the reactor and on all 'sites' if the surface is described by site

fractions. Without this loss mechanism, the plasma simulation will be incorrect and probably non-convergent.

It is generally agreed that a positive ion colliding with a surface will neutralize with 100% probability. The rate at which neutralization processes occur, then, is equal to the total ion flux to the surface. The ion flux is thereby transport-limited and is determined by the ion density and ion velocity at the plasma-sheath boundary. For many of the plasmas considered here, the ion transport through the sheath can be considered as nearly collisionless. According to the Bohm criteria, then, the ion velocity at the plasma-sheath boundary is given by the following relationship

$$U_i \geq U_{i,\text{Bohm}} = \left(\frac{k_B T_e}{m_i} \right)^{1/2} \quad (6)$$

The relationship in Eq. (6) is valid for electropositive discharges. In the presence of negative ions, this relationship should be modified as follows [79]

$$U_i \geq U_{i,\text{Bohm,mod}} = \left(\frac{k_B T_e}{m_i} \right)^{1/2} \left[\left(\frac{n_n}{n_e + n_n} \right) \left(\frac{T_i}{T_e} \right)^{1/2} + \left(\frac{n_e}{n_e + n_n} \right) \right] \quad (7)$$

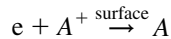
where n_n is the total negative ion density and n_e is the electron density. In the limit of a purely electronegative discharge, the ion flux depends on the ion's thermal velocity.

The CHEMKIN Collection formalism allows explicit application of the Bohm-flux limitation to the reaction-rate parameters for an ion-surface reaction, using the equality in Eq. (6). Furthermore, the result of an ion-surface collision may comprise a number of different possible outcomes. Analogous to the use of 'sticking coefficients,' then, probabilities may be specified for the different reaction paths that result from an ion-surface collision, provided that the total ion fluxes sum to no more than the Bohm flux.

While the Bohm flux indicates the maximum ion flux to a surface, the actual flux must be determined by the ability of the ions to be transported to the plasma sheath. In a well-mixed reactor model, where the plasma is assumed to be electrically neutral overall and kinetics are assumed to be rate limiting, a factor on the order of 0.6 is usually multiplied by the maximum condition given in Eqs. (6) and (7) to estimate the actual ion flux [80]. This factor derives from the Bohm criterion, which gives the ion energy to be $k_B T_e/2$ at the sheath edge, and the idea that the electron density falls off exponentially between the plasma bulk and the wall. The exponential decay is given as $\exp(-\phi/kT_e)$, where ϕ is the local potential, which is approximately equal to the ion energy entering the sheath. At the charge-neutral sheath edge, then, the ion and electron densities are equal to the density in the plasma bulk multiplied by $\exp(-0.5) \approx 0.6$.

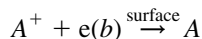
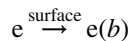
In multidimensional plasma simulations that employ a quasineutral assumption [15,17,18], the maximum Bohm flux becomes the ion's surface loss rate at the plasma/surface boundaries, and the electron flux must be equal to

the sum of the positive ion fluxes. One way to assure this neutrality is to specify the ion recombination reaction as one involving a gas-phase electron, for example



For electropositive discharges, the negative plasma sheath repels negative ions, such that the negative-ion flux to a surface is approximately zero. This condition should be modified, however, if the negative ion density is much greater than the electron density.

For a multidimensional model that includes self-consistent determination of electrostatic fields, through the solution of Poisson's equation, the surface flux condition is handled differently. In this case the electron flux and positive ion flux are not equal at the material surface. The electrons transported to the surface 'stick' with unit probability. Likewise, the ions that get accelerated to the surface by the electric field recombine with a 'surface' electron with a probability of one. However, the charged-species fluxes are determined by the drift and diffusion of electrons and ions to the surface. One method for providing the appropriate surface losses using CHEMKIN software is to define a 'reservoir' of electrons in the bulk material. The electrons add to this reservoir and the ions take an electron from it, as follows



This approach has been used in the 2-dimensional simulation of BCl_3/Cl_2 plasmas [17].

4.2. Neutral chemical reactions at a surface

The chemical reactions of neutral radicals on surfaces in a plasma reactor are similar to those in any chemical vapor deposition system. Only a brief discussion is included here, as Coltrin et al. [2] treat this topic in an accompanying article in this volume. The following types of reactions should be considered: adsorption and desorption of radicals on open or radical surface sites, abstraction of species on the surface by gas-phase radicals, deposition reactions, spontaneous desorption of stable molecules from the surface, etching reactions, and intrasurface-site reactions. Neutral reactions enhanced by the simultaneous bombardment of the surface by ions are described in a separate section below. Reactions may be formulated as individual elementary steps or as 'lumped' reactions that combine the effects of a number of elementary steps. The level of detail usually depends on the amount of information available about the reaction paths and the rate-limiting steps. Reactions of neutral radicals with reactor walls can be especially important in low-pressure systems, often providing critical loss paths in the determination of the radical density near the wafer [81].

The literature on radical reactions at surfaces is quite sparse, which results in the use of many estimates in reaction mechanisms. Examples of experiments addressing plasma radical reactions include work by Ho, Breiland, Buss et al. [82–84], who employed the IRIS (Imaging of Radicals Interacting with Surfaces) technique to measure reactivity of plasma-generated radicals on different surfaces. This technique uses molecular-beam sampling of a plasma and laser-induced fluorescence detection of the beam colliding with a surface. Kota and Graves have also used high-vacuum beam experiments to determine values for radical reaction probabilities on selected surfaces [85].

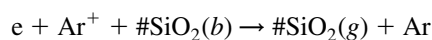
4.3. Ion sputtering

High-energy ions bombarding a surface may cause physical sputtering. Sputtering is an important process in the filling of trenches for inter-metal-layer dielectric deposition, for example, as the sputtering prevents closing off of the trench before the fill is complete [86]. In HDP reactors, the ions in the bulk of the plasma usually have low energy. However, the ion energy at the wafer is often controlled through application of an r.f. bias to the wafer chuck. This bias typically contributes little to the total ionization in the plasma, but directly affects the acceleration of ions towards the wafer surface. Acceleration to high ion energies may result in sputtering, while lower energies are more likely to contribute to ion-enhanced chemical processes. Physical sputtering results from the ion's impact energy being transferred to a surface species, either directly or through collisions in the bulk material, which then desorbs into the gas. The number of molecules that are removed from a surface by a single ion impact is the ion's yield coefficient. The yield coefficient can be described as a function of the ion's energy, as follows

$$y_i = \max\left[a(E_i^b - E_{th}^b)^c, 0\right] \quad (8)$$

where E_i is the ion energy, and E_{th} is a threshold energy for the sputtering process.

This yield formulation is included in the CHEMKIN software. For example, an Argon ion sputtering an SiO_2 molecule from a silicon dioxide bulk material could be described as



YIELD/{a E_{th} b c}/BOHM

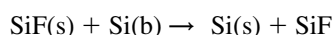
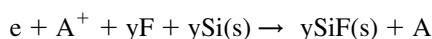
where '#' denotes the yield coefficient, y , with the functional dependence given in Eq. (8). The second line gives the yield parameter values, while the optional CHEMKIN keyword, BOHM indicates the use of the Bohm criterion to determine the reaction's rate of progress. The yield coefficient, together with the rate of progress, determines the rate of production of $\text{SiO}_2(g)$ and the rate of destruction (etching) of $\text{SiO}_2(b)$. Yield coefficients for physical sputtering are determined by well controlled ion-beam experiments [87].

4.4. Ion-enhanced chemical processes

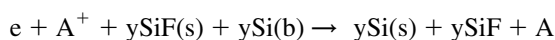
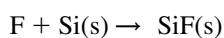
The characteristic process in HDP etching and deposition is low-ion-energy enhancement of chemical reactions. This synergistic process allows for high rates of deposition and etching that are directional with the ion flux. The directionality enables anisotropic filling or etching of microscopic trenches and vias, while the relatively low ion energies avoid the damage of underlying materials that is associated with higher energies. Molecular dynamics simulations have provided important insight into the role of ions in inducing chemical reactions, but have only been applied to a limited number of systems [88]. In most cases, quantitative yield data are derived empirically. Ion-beam studies have generated yield and rate data for fluorine and fluorocarbon etching of silicon and silicon dioxide [89–92], and for chlorine/argon etching of silicon [93,94]. Studies by Cheng et al., reveal additional information regarding the ion-yield dependence on chlorine coverage using in situ measurements in a high-density plasma [95].

Ion-enhanced reactions can be described using a similar formalism to that of physical sputtering, but including a role for reactive neutrals. The combination process may be described as an ion-enhanced adsorption, an ion-enhanced desorption, or a global etch process, as illustrated by the following examples.

(i) Ion-enhanced adsorption followed by etch reaction:



(ii) Chemical adsorption followed by ion-enhanced etch:



(iii) Ion-enhanced chemical etch:



Here, A is an arbitrary atom, 'y' represents the ion's yield function, (s) depicts a surface species, and (b) denotes a species in the bulk material. The above reactions are for example purposes only and are not meant to represent an actual physical process. The choice between the three approaches depends on the amount of information available on the etch process. If the adsorption process is fast and the rate-limiting step is the desorption of etch product, then formulation (ii) is an apt description. If little is known about the relative steps, a global description, such as (iii) is appropriate. Steinbrüchel [96] showed that the ion-energy dependence for ion-induced reaction follows that of direct physical sputtering, as given by Eq. (8), with a direct dependence on the square-root of the ion energy (i.e. $b = 0.5$ and $c = 1.0$).

4.5. Thermodynamic properties

Thermodynamic properties for surface species are generally only important if the surface reactions are cast as reversible processes. In practice, this is rarely done because surface thermochemical properties are not as well defined as those for gas, liquid, or solid phase species, and there are no comparable data compilations. If reverse surface reactions rates are to be determined from equilibrium constants, thermodynamic properties need to be estimated for the all surface species in the mechanism. An example where this level of modeling has been included in a plasma deposition simulation is in the $\text{SiH}_4/\text{O}_2/\text{Ar}$ deposition of SiO_2 [24]. This subject is also discussed by Coltrin et al., in the context of thermal CVD in their accompanying article in this journal [2].

5. Transport properties

In multidimensional plasma simulations, transport properties are important parameters in the equations describing momentum and energy transfer. For weakly ionized plasmas, properties of neutral species may be treated in the same manner as in thermal reacting-flow simulations [23,97,98]. In this case, thermal conductivity, viscosity, and binary diffusion coefficients are related to Stockmayer (or other analytical) potentials that are based on fundamental molecular parameters, such as the Lennard–Jones potential well depth and diameter. Ion and electron transport properties are related to momentum transfer collision frequencies between the charged species and the heavy particles in the discharge. Mixture properties can be calculated either by using mixture-averaged formulas or full multi-component formulations. Mixture-averaged formulas include, for example, the Wilke [99] formula for viscosity, combination averaging for thermal conductivity by Mathur et al. [100], and Fickian diffusion assumptions. More accurate, but also more computationally expensive, are multi-component formulations that require solution of a matrix of equations to determine the mixture properties at each location in the solution domain [23,101,102]. For weakly ionized plasmas, such mixture formulas can include the ion species, as long as the pure-species properties and the binary diffusion coefficients are determined appropriately [103].

For the electrons, the momentum-transfer collision frequencies are calculated from electron-molecule collision cross sections in the same manner as for other collision events. The collision frequency results from the integration of the energy-dependent cross section and a known EEDF, and is thus dependent on the electron temperature. Electron momentum-transfer cross sections are critical data in the evaluation of cross-section sets, because they provide a scaling for electron collisions with a given molecule. Simulations using momentum-transfer collision cross sections are often compared to experimental measurements of drift velocities for validation [28,35].

For ions, collision cross-section data are difficult to find. However, collision frequencies can be derived from polarizability-limited mobility formulas for HDP conditions [104]. In the limit of low electric fields and low temperatures, the mobility of the ion is dominated by polarizability effects, such that

$$\bar{g}_{\text{in}} \bar{\sigma}_{\text{in}}^{\text{mt}} \approx 2\pi \sqrt{\frac{e^2 \alpha_n}{4\pi\epsilon_0 m_{\text{in}}}} \quad (9)$$

Here \bar{g}_{in} is the mean velocity of the ion–neutral collision and $\bar{\sigma}_{\text{in}}^{\text{mt}}$ is the averaged ion–neutral momentum-transfer collision cross section, e is the electron charge, α_n is the polarizability of the neutral molecule, m_{in} is the ion–neutral reduced mass, and ϵ_0 is the free-space permittivity. The product $\bar{g}_{\text{in}} \bar{\sigma}_{\text{in}}^{\text{mt}}$ in this case is a constant function of molecular parameters and can be calculated prior to the plasma simulation. Atomic additivity methods furthermore provide good estimates of molecular polarizabilities, when data are otherwise unavailable [105]. The ion momentum-transfer collision frequency is defined as the product of the neutral molecule density and $\bar{g}_{\text{in}} \bar{\sigma}_{\text{in}}^{\text{mt}}$.

The transport properties of electrons and ions are related to the momentum–transfer collision frequencies as given by the approximate formulas in Table 4 [45]. These relations are valid for weakly ionized plasmas in the presence of small electrostatic fields and neglect the effects of charge–charge collisions.

6. Validation and tuning

Once the reaction mechanisms are assembled from the above parts, the process of obtaining a predictive chemistry set has only begun. The inevitable incompleteness and uncertainty of the reaction-rate parameters makes validation a key component of mechanism development. Uncertainties in the model also arise from approximations contained in the model (e.g. assuming a Maxwellian EEDF), and from the uncertainties in the specified boundary conditions (e.g. accuracy of wall and wafer temperatures).

Diagnostic data can be used to validate model predictions, while sensor data often provide model inlet and boundary condition information. It is highly desirable that validation experiments involve as wide a variety of experiments as is possible. Experiments that separate competing effects are often more useful than those that are designed to closely mimic targeted process conditions. For example, measurements of etch rates on blanket-material wafers allow the step-wise building of mechanisms that enable modeling of patterned wafers containing multiple materials. A large set of comparisons generates more confidence in the model accuracy. Models can extrapolate to regions outside of the validation data only to the extent that the model captures the fundamental and competing processes.

The first test for the model is the ‘reasonable solution’ test. A simulation of typical HDP conditions, for example,

Table 4
Transport–property relations for ions and electrons [45]

Symbol	Property	Formula
ν_{en}	Electron momentum-transfer collision frequency with species n	$n_n \int_0^\infty f(\epsilon) \left(\frac{2\epsilon}{m_e}\right)^{1/2} \sigma(\epsilon) d\epsilon$
ν_{in}	Ion momentum-transfer collision frequency with species n	$n_n \bar{\sigma}_{in}^{mt}$
$\bar{\nu}_{eN}$	Total electron collision frequency with all neutrals	$\sum_n \nu_{en}$
$\bar{\nu}_{iN}$	Total ion collision frequency with all neutrals	$\sum_n \nu_{in} \left(\frac{2m_n}{m_i + m_n}\right)$
λ_e	Electron thermal conductivity	$2.4 \frac{k_B^2 n_e T_e}{m_e \bar{\nu}_{eN}}$
γ_i	Ion-specific-heat ratio	$\frac{c_{pi}}{c_{vi}}$
λ_i	Ion-thermal conductivity	$\left(\frac{9\gamma_i - 5}{\gamma_i - 1}\right) k_B^2 T_i \frac{n_i}{m_i \bar{\nu}_{iN}}$
η_e	Electron viscosity	~ 0
η_i	Ion viscosity	$\frac{4k_B T_i n_i}{\pi \bar{\nu}_{iN}}$
d_{en}	Electron binary diffusion coefficient	$\frac{k_B T_e}{m_e \nu_{en}}$
d_{in}	Ion binary diffusion coefficient	$\frac{k_B T_i}{m_i \nu_{in}}$
μ_e	Electron mobility	$\frac{e}{m_e \bar{\nu}_{eN}}$
μ_i	Ion mobility	$\frac{e}{m_i \bar{\nu}_{iN}}$

should result in electron temperatures of about 2–6 eV and electron densities between 10^{11} and 10^{12} cm^{-3} . An unreasonably high electron temperature may indicate missing collisional energy losses for the electrons, or a saturation of the plasma by species for which a full set of electron collisions have not been included.

The second test for the model is whether or not it can reproduce observed trends in a variety of experiments. The model and chemistry generally have to be adjusted, or reaction paths added, in order to meet this criterion. For example, in recent work on $\text{BCl}_3/\text{Cl}_2/\text{Ar}$ plasmas, it was necessary to add several reactions (e.g. dissociative attachment of BCl and BCl_2) and adjust some rate parameters (by factors of 2–3, well within the uncertainty of kinetics measurements) in order to attain good agreement between model predictions and experiment. In this case the experimental measurements included electron temperatures, electron densities, Cl densi-

ties, and relative BCl and Cl densities [17]. In this process it is important to have a clear understanding of the priority of the trend predictions, the uncertainty in the diagnostic data, the sensitivity of the model results to chemistry parameters, and the uncertainty of the chemistry parameters. A suggested priority of diagnostic data for wafer processing in HDP reactors is (a) direct measures of wafer data, such as etch rate, (b) measurements of etch or deposition precursors, such as ion flux, ion/electron densities, or radical densities, and (c) measurements of intermediates, electron temperature, or wall erosion/deposition data. Sensitivity analysis is very useful for identifying the reaction parameters that most greatly affect the validation comparisons [17].

The final goal of the modeling effort is to provide quantitative predictions of etch and deposition data. Therefore, the goal in mechanism development is not necessarily to pursue the best-possible description of each plausible reaction step, but instead for the mechanism to represent, as a whole, the process of interest, as demonstrated by prediction and verification using an appropriate plasma model. The validation and ‘tuning’ procedure described above is designed to provide the best overall agreement with the available sets of diagnostic data or other observables. This ‘tuning’ process should be constrained to the use of physically-reasonable rate parameters that fall within any known uncertainty limits, which is not equivalent to an ad hoc fitting procedure. A model that contains a number of known fundamental parameters will be more extrapolative and predictive than a model based on an empirical fit to one set of deposition or etching data.

7. Chemistry mechanism reduction

Many of the issues of importance to process and reactor designers, such as questions of deposition or etch uniformity across wafers, require simulations that include a two- or three-dimensional treatment of the plasma transport. The computational resources consumed by such simulations scale with the number of species contained in the reaction mechanism. It is therefore often necessary to reduce the size of a reaction mechanism before transferring it to a higher-order plasma model. This is an area where sensitivity and uncertainty analysis is extremely useful.

Two illustrative examples where detailed gas-phase and surface reaction mechanisms were first developed using a low-order well-mixed reactor model and then successfully reduced for use in 2D plasma simulations are given by Meeks, et al. [17] for $\text{BCl}_3/\text{Cl}_2/\text{Ar}$ chemistry and by Johannes et al. [25] for C_2F_6 etching of SiO_2 . Defining the process window of interest is important to providing a target for the model reduction. For the $\text{BCl}_3/\text{Cl}_2/\text{Ar}$ chemistry, the mechanism was reduced from 22 species to 17. For the C_2F_6 etch chemistry, the mechanism was reduced from 38 species and 206 reactions to 15 species and 50 reactions. In these

cases, etch-rate predictions remained within a few percent of the full model for the targeted set of conditions [25].

8. Conclusions and recommendations

Plasma modeling is capable of addressing practical problems in the microelectronics industry if the appropriate reaction mechanisms are developed. Although this requires many types of data, the problem is tractable. Published examples for $\text{SiH}_4/\text{O}_2/\text{Ar}$ [24], $\text{BCl}_3/\text{Cl}_2/\text{Ar}$ [17], and C_2F_6 [25] plasmas show that, even with many estimated parameters in a simulation, plasma modeling can provide reasonable, quantitative agreement with a wide variety of measurements, as well as give useful insight into the reactor process.

Although the methodology presented here can be used to obtain the needed parameters for reaction mechanism development, the need for continued measurement and computation of electron-impact cross-sections for stable and fragment molecules is paramount. The available knowledge based on low-pressure radical and ion kinetics is also in great need of improvement. Ion and neutral beam experiments, as well as surface-science studies including Fourier-transform infrared (FTIR) spectroscopy, X-ray photoelectron spectroscopy (XPS), and laser-induced fluorescence (LIF) diagnostic techniques also provide valuable ‘fundamental’ and engineering data for modeling of surface processes.

An important lesson from the application of plasma modeling to these complex processing environments is the need for a multidisciplinary approach in broadening the understanding of this area. The synergism between experimental and computational studies can be particularly useful when fundamental knowledge of individual physical and chemical processes is lacking.

Finally, there is a great need for more automated approaches to using uncertainty analysis, sensitivity analysis, parameter estimation, and model optimization. A mathematical treatment of the impact of parameter uncertainty on model results, for example, could greatly facilitate the processes of mechanism development, tuning, and reduction. Also, the compilation and building of reaction mechanisms can be extremely tedious in practice, which points to a need for improved databases and bibliographies of fundamental parameters.

Acknowledgements

P.H. acknowledges the support of Sandia National Laboratories for this work. Sandia is a multiprogram laboratory operated by Sandia Corporation, a Lockheed Martin Company, for the United States Department of Energy under Contract DE-ACO4-94AL85000.

References

- [1] M.A. Lieberman, R.A. Gottscho, in: M. Francombe, J. Vossen (Eds.), *Physics of Thin Films*, Academic Press, New York, 1993.
- [2] M.E. Coltrin, P. Ho, H.K. Moffat, R.J. Buss, *Thin Solid Films* (This issue) 251.
- [3] L.E. Kline, M.J. Kushner, *Crit. Rev. Solid State Mater. Sci.* 16 (This issue) 251.
- [4] G.G. Lister, *J. Appl. Phys.* D 25 (1992) 1649.
- [5] D.B. Graves, *IEEE Trans. Plasma Sci.* 22 (1994) 31.
- [6] D.J. Economou, *Thin Solid Films* (This issue) 348.
- [7] S.C. Deshmukh, D.J. Economou, *J. Appl. Phys.* 72 (1992) 4597.
- [8] C. Lee, D.B. Graves, M.A. Lieberman, D.W. Hess, *J. Electrochem. Soc.* 141 (1993) 1546.
- [9] E. Meeks, J.W. Shon, *IEEE Trans. Plasma Sci.* 23 (1995) 539.
- [10] S. Ashida, C. Lee, M.A. Lieberman, *J. Vac. Sci. Technol. A* 13 (1995) 2498.
- [11] M. Meyyappan, T.R. Govindan, *Vacuum* 47 (1996) 215.
- [12] P.L.G. Ventzek, R.J. Hoekstra, M.J. Kushner, *J. Vac. Sci. Technol. B* 12 (1994) 461.
- [13] R.A. Stewart, P. Vitello, D.B. Graves, *J. Vac. Sci. Technol. B* 12 (1994) 478.
- [14] R.S. Wise, D.P. Lymberopoulos, D.J. Economou, *Appl. Phys. Lett.* 68 (1996) 2499.
- [15] D.P. Lymberopoulos, D.J. Economou, *IEEE Trans. Plasma Sci.* 23 (1995) 573.
- [16] M. Meyyappan, T.R. Govindan, *J. Appl. Phys.* 80 (1996) 1345.
- [17] E. Meeks, P. Ho, A. Ting, R.J. Buss, *J. Vac. Sci. Technol. A* 16 (1998) 2227.
- [18] D.J. Economou, T.J. Bartel, R.S. Wise, D.P. Lymberopoulos, *IEEE Trans. Plasma Sci.* 23 (1995) 581.
- [19] J. Johannes, T.J. Bartel, D.J. Economou, *J. Electrochem. Soc.* 144 (1997) 2448.
- [20] D. Hash, M. Meyyappan, *J. Electrochem. Soc.* 144 (1997) 3999.
- [21] M.D. Kilgore, H.M. Wu, D.B. Graves, *J. Vac. Sci. Technol. B* 12 (1994) 494.
- [22] J. Johannes, T.J. Bartel, D. Sears, J. Payne, *Gemini: A Hybrid Plasma Modeling Capability for Low Pressure Systems. User's Manual - V 1.7*. Sandia National Laboratories Report SAND96-0590, Sandia National Laboratories, 1996.
- [23] R.J. Kee, F.M. Rupley, J.A. Miller, et al., *CHEMKIN Collection, Reaction Design*, San Diego, CA, 1997.
- [24] E. Meeks, R.S. Larson, P. Ho, S.M. Han, E. Edelberg, E. Aydil, C. Apblett, *J. Vac. Sci. Technol. A* 16 (1998) 544.
- [25] J. Johannes, E. Meeks, D. Economou, J. Feldstein (Eds.), *The 29th AIAA Plasma Dynamics and Laser Conference*, 1998.
- [26] D.B. Graves, M.J. Kushner, J.W. Gallagher, A. Garscadden, G.S. Oehrlein, A.V. Pheips, *Database Needs for Modeling and Simulation of Plasma Processing*, National Research Council, Panel of Database Needs in Plasma Processing, 1996.
- [27] L.G. Christophorou, J.K. Olthoff, M.V. Rao, *J. Phys. Chem. Ref. Data* 25 (1996) 1341.
- [28] W.L. Morgan, *Plasma Chem. Plasma Process.* 12 (1992) 477.
- [29] L.G. Christophorou, J.K. Olthoff, *J. Phys. Chem. Ref. Data* 27 (1998) 1.
- [30] L.G. Christophorou, J.K. Olthoff, M.V. Rao, *J. Phys. Chem. Ref. Data* 26 (1997) 1.
- [31] L.G. Christophorou, J.K. Olthoff, Y. Wang, *J. Phys. Chem. Ref. Data* 26 (1997) 1205.
- [32] L.G. Christophorou, J.K. Olthoff, *J. Phys. Chem. Ref. Data* 27 (1998) 889.
- [33] Y. Itikawa, A. Ichimura, K. Onda, et al., *J. Phys. Chem. Ref. Data* 18 (1989) 23.
- [34] Y. Itikawa, A. Ichimura, *J. Phys. Chem. Ref. Data* 19 (1990) 637.
- [35] W.L. Morgan, *Plasma Chem. Plasma Process.* 12 (1992) 449.
- [36] J. Perrin, O. Leroy, M.C. Borge, *Contrib. Plasma Phys.* 36 (1996) 3.

- [37] R.K. Janev, W.D. Langer, K. Evans, D.E. Post, *Elementary Processes in Hydrogen-Helium Plasmas*, Springer, New York, 1987.
- [38] A.V. Phelps, R.J. Van Brunt, *J. Appl. Phys.* 64 (1988) 4269.
- [39] T.J. Sommerer, M.J. Kushner, *J. Appl. Phys.* 71 (1992) 1654.
- [40] J.D. Bukowski, D.B. Graves, P. Vitello, *J. Appl. Phys.* 80 (1996) 2614.
- [41] E. Meeks, R.S. Larson, S.R. Vosen, J.W. Shon, *J. Electrochem. Soc.* 144 (1997) 358.
- [42] K.L. Bell, H.B. Gilbody, J.G. Hughes, A.E. Kingston, F.J. Smith, *J. Phys. Chem. Ref. Data* 12 (1983) 891.
- [43] M.A. Lennon, K.L. Bell, H.B. Gilbody, et al., *J. Phys. Chem. Ref. Data* 17 (1988) 1285.
- [44] R.S. Freund, R.C. Wetzel, R.J. Shul, T.R. Hayes, *Phys. Rev. A* 41 (1990) 3575.
- [45] M. Mitchner, C.H. Kruger, *Partially Ionized Gases*, Wiley, New York, 1973.
- [46] L.G. Christophorou, *Electron-Molecule Interactions and Their Applications*, Academic Press, New York, 1984.
- [47] J.-L. Delcroix, D. Humbert and C. Leprince, GAPHYOR, A Database for Atoms, Molecules, Gases and Plasmas, Laboratoire de Physique des Gaz et des Plasmas: <http://gaphyor.lpgp.u-psud.fr/gaphyor/gaphyor.html> (Orsay, 1998).
- [48] J.K. Olthoff, *Electron Interactions with Plasma Processing Gases*, National Institute of Standards and Technology: <http://www.eeel-nist.gov/811/refdata/index.html> (Washington, DC, 1998).
- [49] W.L. Morgan and W.K. Trail, *Graphical Java Cross Section and Reaction Rates Database*, Kinema Research, Inc.: <http://www.kinema.com/kinema> (Monument, CO, 1998).
- [50] W. Huo, *Electron-molecule Collision Cross Sections*, NASA-Ames: <http://www.ipt.arc.nasa.gov/databasemenu.html> (Moffett Field, CA, 1998).
- [51] S.E. Stein, *NIST Standard Reference Database 25: NIST Structures and Properties*, U.S. Department of Commerce, Gaithersburg, MD, 1994.
- [52] M.W. Chase, C.A. Davies, J.R. Downey, D.J. Frurip, R.A. McDonald, A.N. Syverud, *J. Phys. Chem. Ref. Data* 14 (Suppl. 1) (1985) 1.
- [53] K.P. Huber, G. Herzberg, *Molecular Spectra and Molecular Structure IV. Constants of Diatomic Molecules*, Van Nostrand Reinhold, New York, 1979.
- [54] P. Ahlrichs, U. Riedel, J. Warnatz, *J. Vac. Sci. Technol. A* 16 (1998) 1560.
- [55] R.G. Gilbert, K. Luther, J. Troe, *Ber. Bunsenges. Phys. Chem.* 87 (1983) 169.
- [56] K.A. Holbrook, M.J. Pilling, S.H. Robertson, *Unimolecular Reactions*, Wiley, New York, 1996.
- [57] F. Westley, D.H. Frizzell, J.T. Herron, R.F. Hampson, W.G. Mallard, *NIST Chemical Kinetics Database, NIST Standard Reference Database*, 17, U.S. Department of Commerce, Gaithersburg, MD, 1993.
- [58] V.N. Kondratiev, *Rate Constants of Gas Phase Reactions (COM-72-J0014)*, U.S. Department of Commerce, Washington, DC, 1972.
- [59] V.G. Anicich, *J. Phys. Chem. Ref. Data* 22 (1993) 1469.
- [60] J.M. Farrar, *Annu. Rev. Phys. Chem.* 46 (1995) 525.
- [61] A.V. Phelps, *J. Phys. Chem. Ref. Data* 21 (1992) 883.
- [62] B.L. Kickel, J.B. Griffin, P.B. Armentrout, *Zeitschr. Phys. D* 24 (1992) 101.
- [63] C.Q. Jiao, R. Nagpal, P. Haaland, *Chem. Phys. Lett.* 265 (1997) 239.
- [64] C.Q. Jiao, R. Nagpal, P.D. Haaland, *Chem. Phys. Lett.* 269 (1997) 117.
- [65] B.M. Smirnov, *Negative Ions*, McGraw-Hill, New York, 1982.
- [66] B.J. McBride, *Thermodynamic Properties to 6000 K for 210 Substances: NASA Lewis Report SP-3001*, NASA, 1963.
- [67] P. Ho, C.F. Melius, *J. Phys. Chem.* 94 (1990) 5120.
- [68] P. Ho, C.F. Melius, *J. Phys. Chem.* 99 (1995) 2166.
- [69] M.D. Allendorf, C.F. Melius, *J. Phys. Chem.* 101 (1997) 2670.
- [70] P. Ho, M.E. Colvin, C.F. Melius, *J. Phys. Chem.* 101 (1997) 9470.
- [71] M.E. Coltrin, R.J. Kee, F.M. Rupley, *Int. J. Chem. Kinet.* 23 (1991) 1111.
- [72] M.E. Coltrin, R.J. Kee, F.M. Rupley, E. Meeks, *SURFACE CHEM-KIN III: A Fortran Package for Analyzing Heterogeneous Chemical Kinetics at a Solid-Surface-Gas-Phase Interface*, Sandia National Laboratories Report SAND96-8217, Sandia National Laboratories, 1996.
- [73] E. Meeks, H.K. Moffat, J.F. Grcar, R.J. Kee, *AURORA: A Fortran Program for Modeling Well Stirred Plasma and Thermal Reactors with Gas and Surface Reactions*, Sandia National Laboratories Report SAND96-8218, Sandia National Laboratories, 1996.
- [74] J.W. Coburn, *IEEE Trans. Plasma Sci.* 19 (1991) 1048.
- [75] J.W. Coburn, H.F. Winters, *Appl. Surf. Sci.* 22/23 (1985) 63.
- [76] D.W. Hess, *J. Vac. Sci. Technol. A* 8 (1990) 1677.
- [77] G.S. Oehrlein, *Surf. Sci.* 386 (1997) 222.
- [78] L.-Y. Cheng, J.P. McVittie, K.C. Saraswat, *Appl. Phys. Lett.* 58 (1991) 2147.
- [79] N.S.J. Braithwaite, J.E. Allen, *J. Phys. D* 21 (1988) 1733.
- [80] M.A. Lieberman, A.J. Lichtenberg, *Principles of Plasma Discharges and Materials Processing*, Wiley, New York, 1994.
- [81] E. Meeks, J.W. Shon, *J. Vac. Sci. Technol. A* 13 (1995) 2884.
- [82] P. Ho, W.G. Breiland, R.J. Buss, *J. Chem. Phys.* 91 (1989) 2627.
- [83] R.J. Buss, P. Ho, M.E. Weber, *Plasma Chem. Plasma Process.* 13 (1993) 61.
- [84] E.R. Fisher, P. Ho, W.G. Breiland, R.J. Buss, *J. Phys. Chem.* 96 (1992) 9855.
- [85] G.P. Kota, D.B. Graves, *J. Vac. Sci. Technol. A* (1997).
- [86] S.E. Lassig, J. Li, J.P. McVittie, C. Apblett (Eds.), *DUMIC Conference 101D/95/0190 ISMIC*, 1995.
- [87] H.H. Anderson, H.L. Bay, in: R. Behrisch (Ed.), *Sputtering by Particle Bombardment I. Physical Sputtering of Single-Element Solids*, Springer, New York, 1981, p. 145.
- [88] M.E. Barone, D.B. Graves, *J. Appl. Phys.* 77 (1995) 1263.
- [89] J.W. Coburn, *J. Vac. Sci. Technol. B* 12 (1994) 1384.
- [90] J.W. Butterbaugh, D.C. Gray, H.H. Sawin, *J. Vac. Sci. Technol. B* 9 (1991) 1461.
- [91] D.C. Gray, I. Tepermeister, H.H. Sawin, *J. Vac. Sci. Technol. B* 11 (1993) 1243.
- [92] N. Hershkowitz, H.L. Maynard, *J. Vac. Sci. Technol. A* 11 (1993) 1172.
- [93] M. Balooch, M. Moalem, A.V. Hamza, *J. Vac. Sci. Technol. A* 14 (1996) 229.
- [94] J.P. Chang, H.H. Sawin, *J. Vac. Sci. Technol. A* 15 (1997) 610.
- [95] C.C. Cheng, K.V. Guinn, V.M. Donnelly, I.P. Herman, *J. Vac. Sci. Technol. A* 12 (1994) 2630.
- [96] C. Steinbruechel, *Appl. Phys. Lett.* 55 (1989) 1960.
- [97] J.O. Hirschfelder, C.F. Curtiss, R.B. Bird, *Molecular Theory of Gases and Liquids*, Wiley, New York, 1967.
- [98] L. Monchick, E.A. Mason, *J. Chem. Phys.* 35 (1961) 1676.
- [99] C.R. Wilke, *J. Chem. Phys.* 18 (1950) 517.
- [100] S. Mathur, P.K. Tondon, S.C. Saxena, *Mol. Phys.* 12 (1967) 569.
- [101] G. Dixon-Lewis, *Proc. R. Soc. A* 304 (1968) 111.
- [102] G. Dixon-Lewis, in: W.C. Gardiner (Ed.), *Combustion Chemistry*, Springer, New York, 1984.
- [103] U. Daybelge, PhD thesis, Stanford University, 1968.
- [104] E.W. McDaniel, E.A. Mason, *The Mobility and Diffusion of Ions in Gases*, Wiley, New York, 1973.
- [105] M.E. Riley, personal communication, Estimates of transport coefficients or ions in BCl_3 and other species, 1996